Optimization of Precoder and Combiner in mmWave Hybrid Beamforming Systems for Multi-user Downlink Scenario

Abdul Haq Nalband[1*], Mrinal Sarvagya[2], and Mohammed Riyaz Ahmed[1]

[1] School of Multidisciplinary Studies, REVA University, Bengaluru, India
[2] School of Electronics and Communication Engineering, REVA University, Bengaluru, India
[*] Corresponding author. E-mail: abdulhaq@reva.edu.in

Received: Oct. 02, 2020; Accepted: June. 24, 2021

Beamforming at millimeter wave (mmWave) band, promises to significantly support 5G networks in achieving their performance goals. The conventional digital beamforming uses a separate RF chain for each antenna element, while it leads to high cost and hardware complexity in mmWave massive MIMO antenna systems. Beamforming with multiple data streams called precoding improves the system's spectral efficiency and one of its kind hybrid beamforming reduces the cost and overcomes the hardware limitation by using reduced number of RF chains. This work considers, transmit precoding, receive combining in mmWave hybrid beamforming systems and constructs a dictionary matrix containing array response vectors. This paper proposes an extended simultaneous orthogonal matching pursuit (ESOMP) algorithm to compute the block-sparse matrix. The non-zero rows of block-sparse matrix and dictionary matrix are further processed to achieve precoder/combiner optimization in multi-user downlink scenario. Simulation results reveal that the proposed method performs close to the ideal digital beamforming scheme while improving the spectral efficiency when compared to the state-of-the-art algorithm.

Keywords: 5G, Beamforming, Hybrid Precoding, mmWave, Massive MIMO

http://dx.doi.org/10.6180/jase.202204_25(2).0002

1. Introduction

The new wireless technology-5G enables a new type of network that is aimed to connect virtually everything including devices, objects, and machines. 5G promises to render higher multi-Gbps peak data rates, ultra-low latency, high reliable connectivity, massive network capacity, and a more stable user experience to large users [1]. Millimeter-wave (30GHz - 300GHz) band occupies a large unlicensed bandwidth and significantly contributes to 5G systems in achieving the aforementioned promises [2]. Nevertheless, mmWave signals pose greatly reduced transmission distance, higher path loss, and sensitivity to blockage [3]. The large scale antenna array system called massive MIMO is essential to mitigate the severe penetration loss and path loss of mmWaves [4]. The signal transmission range can further be increased by beamforming techniques. Beamforming prepares the antennas to focus their transmissions only in desired directions.

However, the advent of mmWave technology substantially increases the size of antenna array (massive MIMO) which puts considerable practical constraints on beamforming. However, full digital beamforming (DBF) demands a separate RF chain dedicated to every antenna element, this leads to greater power consumption, unaffordable cost of deployment, and greater hardware complexity for mmWave massive MIMO systems [5]. Hybrid beamforming schemes have been proposed as a replacement to digital beamforming because of their potential to use a reduced number of RF chains which in turn reduce the power consumption, cost, and hardware complexity of the system while guaranteeing sufficient beamforming gain [6].

In hybrid beamforming architectures, the precoding (at transmitter) or combining (at receiver) process is split into a small-sized baseband digital beamformer (where a reduced quantity of RF chains used mitigate the interference) and a greater size analog beamformer (a large quantity of analog phase shifters are used to improve the beamforming gain). However, the optimal hybrid beamforming scheme needs to solve an intractable non-convex optimization problem that involves combined optimization over the four matrix variables, that is, the hybrid precoding and combining matrices.

Many hybrid beamforming schemes have been proposed to maximize spectral efficiency [7, 8]. For example, the authors in [9] formed the hybrid beamforming problem as a sparse reconstruction problem, and then used the orthogonal matching pursuit (OMP) method to compute the near optimal precoder and combiner. Though the OMP based hybrid transceiver design exhibits reasonably stable performance, the performance deviation is seen between the existing OMP based method and the full digital beamforming architecture. The work in [10] further improved the spectral efficiency to approach fully digital beamforming by using an alternating minimization algorithm instead of the OMP algorithm but yet not close to the performance of DBF.

The Hybrid Beamforming scheme collectively computes the baseband precoding and RF beamforming weights using the channel matrix. The simultaneous orthogonal matching pursuit (SOMP) algorithm based on compressive sensing mechanism is discussed in [11] that examines the characteristics of sparsity due to channel scatterings and determines the non-zero vectors to generate the RF beamforming weights. Many researchers have used the SOMP algorithm to design, a cost-effective and more efficient hybrid beamforming algorithms [12], but lacks in enhancing the bit error rate (BER) performance.

The efficiency of the spectrum and the BER are two primary optimization objectives for hybrid beamforming problems [13, 14]. However, many challenges have emerged from maximizing spectral efficiency and reducing the BER under the limitations reaped from the mmWave hybrid architecture. This work solves this problem by jointly designing the analog (RF) and digital (baseband) precoder and combiner. The objectives are achieved by employing the following contributions to this work.

- The entire coverage area of the transmitter is partitioned into angular grids. The transmit array response matrix is determined by constructing a dictionary matrix by considering the angular grids.

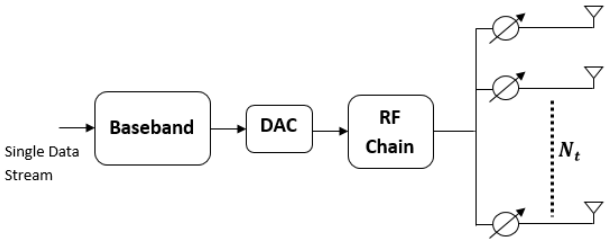

Fig. 1. Analog Beamforming

- The precoder optimization problem is formulated by estimating a block sparse matrix. The optimal baseband precoder is determined by extracting the non-zero rows from the block sparse matrix. The RF precoder is formed from the columns of the array response matrix which corresponds to the non-zero rows of the block spark matrix

- The RF combiner is determined from the receive array response matrix which is computed using the least-squares solution. The baseband combiner is formed by processing the RF combiner along with the channel covariance matrix.

- The proposed scheme is employed for a uniform linear and planar array antenna systems and the performance is presented for both the antenna systems.

2. Beamforming Architectures

The analog beamforming (ABF) is shown in Fig. 1 uses a single RF chain and the number of RF phase shifters equal to the number of antenna elements. The ABF is simple to implement, consumes less power, lower cost, and lower hardware complexity. But ABF possess the supplementary restrictions and does not allow spatial multiplexing, making it impossible to form multiple beams. An RF chain can produce a single beam in a cycle, hence the ABF system can serve only one data stream/user. Therefore, ABF cannot enhance the efficiency of the spectrum. These restrictions in ABF make a rejection of its application in a multi-user scenario.

Traditional MIMO systems usually operate with digital beamforming (DBF) performed at baseband controlling the amplitude and phase of the signals. The DBF can generate multiple beams and support multiuser communications [15, 16]. However, digital beamforming is shown in Fig. 2, requires not just a dedicated processor, but also a separate RF chain for individual antenna element. At mmWave frequency, when massive MIMO antennas are used, the high power consumption, cost, and hardware complexity of the DBF system make it unaffordable to deploy in

practice. Therefore, mmWave massive MIMO systems rely profoundly on beamforming at the RF stage [17]. The RF beamforming at the base station and RF combining at the user equipment can be realized using analog phase shifters that control the phase of the transmitted/received signal at every element of antenna array [18, 19].

For a more favorable tradeoff among the performance and costs, the HBF approach that combines the advantages ABF and flexibility of DBF is most suitable for mmWave MIMO systems. The HBF renders the performance close to the full digital beamforming while reducing the power requirement and complexity of the hardware. Because of this reason, the HBF has been into thick research [20, 21]. The other clear advantage of deploying hybrid architecture is the reduction of the required resolution of the ADC units used before the RF chains in the transmitter system.

3. System Model and Problem Formulation

3.1. System Model

We consider a multi-user downlink scenario, where multiple users are being served by a single base station (BS). The antenna system of both, the BS and user terminals needs to be employing the HBF technique. We assume mmWave hybrid precoding/combining system as shown in Fig. 4. The transmitter i.e., BS is equipped with N_t antennas and N_t^{RF} RF chains to transmit N_s data streams over the channel simultaneously, whereas a receiver i.e, mobile station (MS) employs N_r antennas and N_r^{RF} RF chains for the reception. It is important that $N_s \leq N_t^{RF} \leq N_t$ and $N_s \leq N_t^{RF} \leq N_t$ to support such a multi-stream scenario. However, N_s can be also be referred to as the number of user terminals. The signal received at the user terminal before combining can be represented as presented in [22].

$$Y = X \times F \times H + n \tag{1}$$

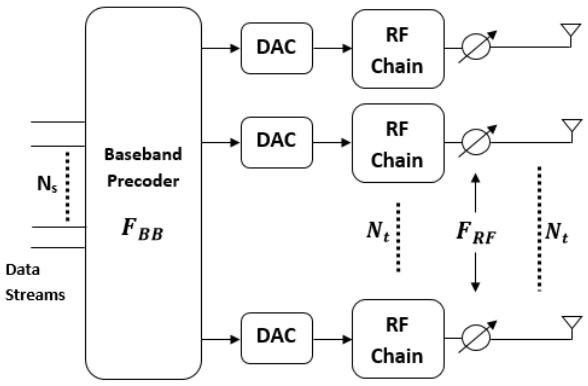

Fig. 2. Digital Beamforming

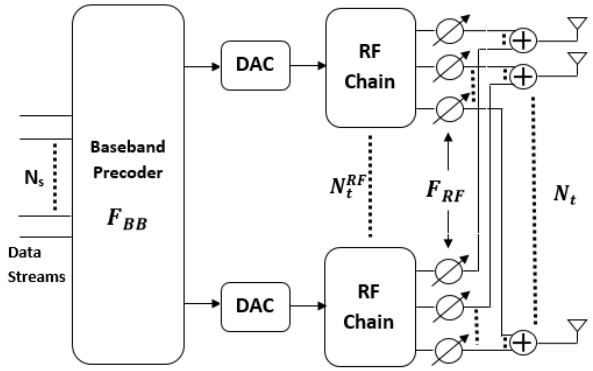

Fig. 3. Hybrid Beamforming

Here X is the input data matrix having N_s columns, each representing a data stream. F is a precoding matrix with dimensions $N_s \times N_t$. H is the mmWave channel matrix. The matrix n, having $N_r$columns representing the receiver noise at each antenna element. The received signal is further processed and recovered through combining weights. The recovered signal is written as described in [22].

$$\hat{Y} = (X \times F \times H + n)W \tag{2}$$

Where W is a $N_r \times N_s$ matrix of combining weights. The data stream can be recovered independently as the product of precoding and combining weights $F \times H \times W'$ results in a diagonal matrix. The precoding and the combining weights are computed by jointly processing the baseband (digital) weights represented as F_{bb} and RF (analog) weights represented as F_{RF}. However the baseband and RF beamforming weights are computed independently. The baseband beamforming weights process the input data streams and pass signals to every RF chain, then the RF beamforming weights control the signals phase using analog phase shifters, achieve the directional transmission and reception. Therefore, we have $F = F_{BB} \times F_{RF}$ and $W = W_{BB} \times W_{RF}$.

3.2. MmWave MIMO channel Model

The mmWave channels render limited scattering. Considering this characteristics, the channel model include L_u independent multi paths for each H_k [13, 14], where $L_u < N_t$ for limited scattering. Then the channel between BS and each UE can be represented as

$$H_k = \sqrt{\frac{N_t N_r^k}{L_u}} \sum_{l=1}^{L_u} \alpha_{k,l} \cdot a_{UE}\left(\theta_{k,l}^{UE}, \varnothing_{k,l}^{UE}\right) a_{BS}^{H}\left(\theta_{k,l}^{BS}, \varnothing_{k,l}^{BS}\right) \tag{3}$$

,where $\alpha_{k,l}$ is the complex path coefficient and is considered to follow the standard i.i.d complex Gaussian distribution

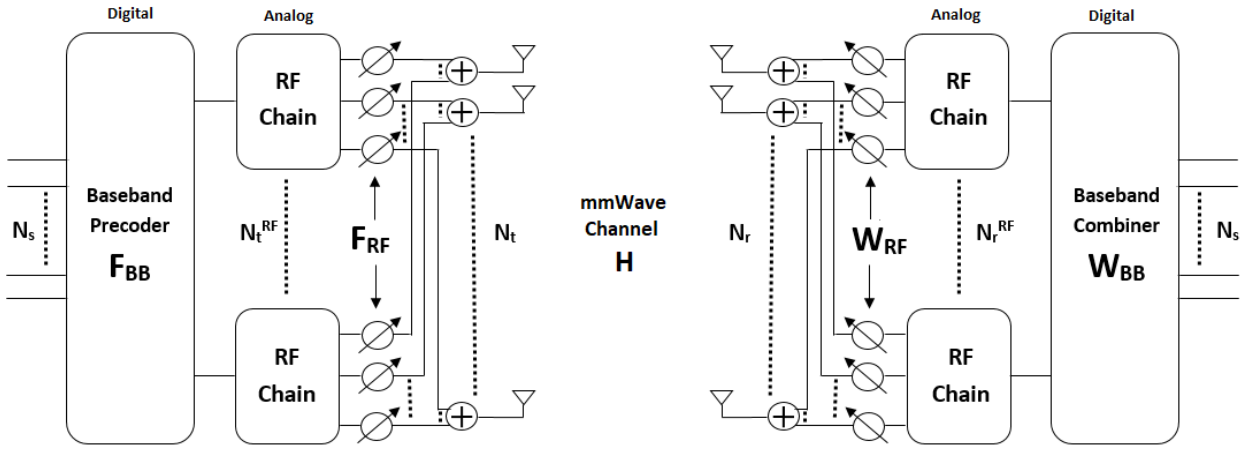

Fig. 4. mmWave Hybrid Beamforming System

that produce the Rayleigh component. $a_{UE}(\theta_{k,l}^{UE}, \varnothing_{k,l}^{UE})$ and $a_{BS}^{H}(\theta_{k,l}^{BS}, \varnothing_{k,l}^{BS})$ are array response vectors at receiver and transmitter respectively, where $\theta_{k,l}^{UE}(\varnothing_{k,l}^{UE})$ and $\theta_{k,l}^{BS}(\varnothing_{k,l}^{BS})$ azimuth (elevation) angles of arrival and departure (AoAs/AoDs) of l^{th} path. For uniform linear arrays (ULAs), only the azimuth AOAs and AoDs are considered and the array response vector is given by

$$H_k = \sqrt{\frac{N_t N_r^k}{L_u}} \sum_{l=1}^{L_u} \alpha_{k,l} \cdot a_{UE}\left(\theta_{k,l}^{UE}, \varnothing_{k,l}^{UE}\right) a_{BS}^{H}\left(\theta_{k,l}^{BS}, \varnothing_{k,l}^{BS}\right) \tag{4}$$

,where $k = 2\pi/\lambda$ with λ as wavelength of the carrier signal, and dis the spacing between the antenna elements. For uniform planar array antennas, the array response vector is given by

$$a_{UPA}(\theta, \phi) = \frac{1}{\sqrt{N}} \left[1, e^{jkd(m\sin(\phi)\sin(\theta)+n\cos(\theta))}, \ldots, e^{jkd((W-1)\sin(\varnothing)\sin(\theta)+(H-1)\cos(\theta))}\right]^T \tag{5}$$

,where $0 \leq m \leq W-1, 0 \leq n \leq H-1$, and $N = WH$. $N = N_t$ for a_{BS} and $N = N_r^k$ for a_{UE} of H_k.

3.3. Problem Formulation

The traditional MIMO channel can be decomposed as $H = U\sum V^H$, where the matrices U and V are semi-Unitary such that $U^H U = I$ and $V^H V = I$ and $\sum$ is the diagonal matrix of non-negative values. For the classical MIMO, we can set the baseband precoder equal to V and RF precoder to I or they can even be interchanged. But for mmWave massive MIMO the ideal baseband/RF precoder must be set to $A_t V$. The transmit array response vectors in transmit array matrix A_t form a basis for the column space of H^H. The matrix A_t need to be estimated either by constructing a dictionary matrix or by applying the principle of scattering. Therefore, the best precoder approximation problem can be formulated as $\arg\max_{F_{BB}} \left\| V - \mathbf{A_t}\widetilde{\mathbf{F_{BB}}} \right\|_F^2$. At the receiver the received vector Y is acted upon by combining weights. The combiner weights need to be computed so as to reduce the minimum mean square error (MMSE) of the receiver. The HBF system aims to deliver greater spectral efficiency, the precoding and combining weights decides the performance of the HBF system. Therefore, the optimization problem is formulated so to optimally compute these weights. As the RF beamforming and combining coefficients are used only to control the direction of beams, there are few additional constraints in the optimization problem to compute these weights. Theoretically, the combination of $F_{BB} \times F_{RF}$ and $W_{BB} \times W_{RF}$ that are produced by the HBF method are expected to be near estimates of F and W which are computed without any constraints.

4. Proposed Extended Simultaneous Orthogonal Matching Pursuit Method

In this section, we discuss an effective mechanism that considers the beam grids for computing the array response matrices. Subsequently, we propose an extended simultaneous orthogonal matching pursuit algorithm (ESOMP). The transmit array response matrix can be constructed by considering the angular grid $\varnothing_T$ of size G , with $\theta \epsilon \varnothing_T$, $1 \leq i \leq G$ and $G \geq N_t$. The dictionary matrix A is constructed as in Eq. (3).

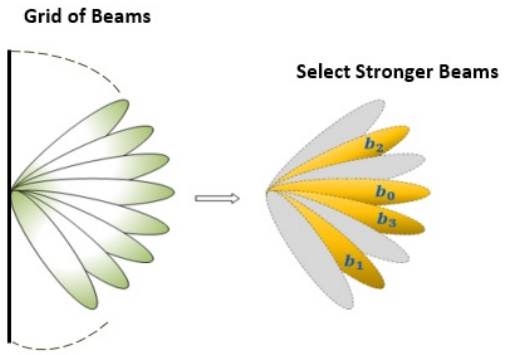

Fig. 5. Angular grids

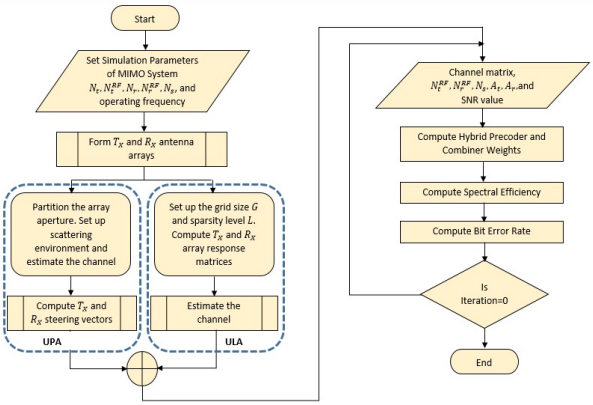

Fig. 6. Flow chart of research method

$$\mathbf{A} = [\mathbf{a}(\boldsymbol{\theta_1})\,\mathbf{a}(\boldsymbol{\theta}_2)\,\mathbf{a}(\boldsymbol{\theta}_3)\ldots\mathbf{a}(\boldsymbol{\theta_G})]$$
$$\mathbf{a}(\boldsymbol{\theta_l}) = \begin{bmatrix} \mathbf{1} \\ \mathbf{e}^{-\mathbf{j}\frac{2\pi}{\lambda}\mathbf{d}\cos\theta_1} \\ \vdots \\ \mathbf{e}^{-\mathbf{j}\frac{2\pi}{\lambda}(\mathbf{N_t}-\mathbf{1})\mathbf{d}\cos\theta_1} \end{bmatrix} \tag{6}$$

Fig. 5 represents the formation of angular beam grids across the entire region of coverage. The transmitter system selects only the specified number of directions in which beams are stronger and receivers are located. The transmission occurs only on those selected directions. This selection of stronger beams happens accurately if the precoder is designed with the best approximation. The precoder optimization problem is formulated by estimating a block sparse matrix. The optimal baseband precoder is determined by extracting the non-zero rows from the block sparse matrix. The RF precoder is formed from the columns of the array response matrix which corresponds to the non-zero rows of the block spark matrix. The RF combiner is determined from the receive array response matrix which is computed using the least-squares solution. The baseband combiner is formed by processing the RF combiner along with the channel covariance matrix. The optimization of precoder (baseband and RF precoding) and combiner (RF combining and baseband combining) can be achieved through the proposed scheme as illustrated in the algorithm. The proposed scheme is employed for a uniform linear and planar array antenna systems and the performance is presented for both the antenna systems. The flow of research method is as depicted in the flow chart of Fig. 6.

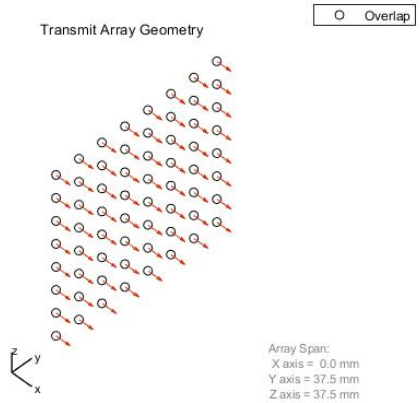

Fig. 7. UPA geometry at BS

Algorithm 1. Proposed Extended SOMP Algorithm: Precoder Optimization

$\mathbf{F}_{\mathrm{RF}}^{(0)} = [\,]$,
$[\mathbf{U}, \mathbf{S}, \mathbf{V}] = \mathrm{svd}(\mathbf{H}), \mathbf{F_{ovt}} = \mathbf{V}(:, 1:\mathrm{N_s})$
$\mathbf{F}_{\mathrm{res}}^{(0)} = \mathbf{F_{opt}}$
for $1 \le k \le N_t^{RF}$ **do**

$$\psi = \mathbf{A}_{\mathrm{t}}^{\mathrm{H}}\mathbf{I}_{\mathrm{Nt}}\mathbf{F}_{\mathrm{res}}^{(\mathrm{k}-1)}$$
$$\mathrm{i(k)} = \mathrm{agr\,max}\left[\Psi\Psi^{\mathrm{H}}\right]_{1,1}$$
$$\mathbf{F}_{\mathrm{RF}}^{(\mathrm{k})} = \mathbf{A}_{\mathrm{t}}[:, \mathrm{i(k)}]$$
$$\mathbf{F}_{\mathrm{BB}}^{(\mathrm{k})} = \left(\left(\mathbf{F}_{\mathrm{RF}}^{(\mathrm{k})}\right)^{\mathrm{H}}\mathbf{F}_{\mathrm{RF}}^{(\mathrm{k})}\right)^{-1}\left(\mathbf{F}_{\mathrm{RF}}^{(\mathrm{k})}\right)^{\mathrm{H}}\mathbf{F}_{\mathrm{opt}}$$
$$\mathbf{F}_{\mathrm{res}}^{(\mathrm{k})} = \frac{\mathbf{F}_{\mathrm{opt}} - \mathbf{F}_{\mathrm{RF}}^{(\mathrm{k})}\mathbf{F}_{\mathrm{BB}}^{(\mathrm{k})}}{\left\|\mathbf{F}_{\mathrm{opt}} - \mathbf{F}_{\mathrm{RF}}{}^{(\mathrm{k})}\mathbf{F}_{\mathrm{BB}}(\mathrm{k})\right\|_{\mathrm{F}}}$$

end
$\mathbf{F}_{\mathrm{BB}} = \frac{\sqrt{\mathrm{N_s}}\mathbf{F}_{\mathrm{BB}}}{\|\mathbf{F}_{\mathrm{RF}}\mathbf{F}_{\mathrm{BB}}\|_{\mathrm{F}}}$
$\mathbf{F}_{\mathrm{BB}} = \mathbf{F}_{\mathrm{BB}}^{\mathrm{T}}, \mathbf{F}_{\mathrm{RF}} = \mathbf{F}_{\mathrm{RF}}^{\mathrm{T}}$

Algorithm 2. Proposed Extended SOMP Algorithm: Combiner Optimization

$\mathbf{W}_{\mathrm{RF}}^{(0)} = [\,]$,
$\mathbf{W}_{\mathrm{res}}^{(0)} = \mathbf{W}_{\mathrm{MMSE}}$
$\mathbf{R}_{\mathrm{SS}} = \mathbf{I}_{\mathrm{N_s}}, \mathbf{R}_{\mathrm{YY}} = \mathbf{H}\mathbf{F}_{\mathrm{RF}}\mathbf{F}_{\mathrm{BB}}\mathbf{R}_{\mathrm{SS}}\mathbf{F}_{\mathrm{BB}}^{\mathrm{T}}\mathbf{H}^{\mathrm{T}} + \mathrm{SNR}^2\mathbf{I}_{\mathbf{N_r}}$
for $1 \leq k \leq N_r^{RF}$ **do**

$$\psi = \mathbf{A}_{\mathrm{r}}^{\mathrm{H}}\mathbf{R}_{\mathrm{YY}}\mathbf{W}_{\mathrm{res}}^{(\mathrm{k}-1)}$$

$$\mathrm{i(k)} = \mathrm{agr\,max}\left[\Psi\Psi^{\mathrm{H}}\right]_{1,1}$$

$$\mathbf{W}_{\mathrm{RF}}^{(\mathrm{k})} = \mathbf{A}_{\mathrm{r}}[:, \mathrm{i(k)}]$$

$$\mathbf{W}_{\mathrm{BB}}^{(\mathrm{k})} = \left(\left(\mathbf{W}_{\mathrm{RF}}^{(\mathrm{k})}\right)^{\mathrm{H}}\mathbf{R}_{\mathrm{YY}}\mathbf{W}_{\mathrm{RF}}^{(\mathrm{k})}\right)^{-1}\left(\mathbf{W}_{\mathrm{RF}}^{(\mathrm{k})}\right)^{\mathrm{H}}\mathbf{R}_{\mathrm{YY}}\mathbf{W}_{\mathrm{MMSE}}$$

$$\mathbf{W}_{\mathrm{res}}^{(\mathrm{k})} = \frac{\mathbf{W}_{\mathrm{MMSE}} - \mathbf{W}_{\mathrm{RF}}^{(\mathrm{k})}\mathbf{W}_{\mathrm{BB}}^{(\mathrm{k})}}{\left\|\mathbf{W}_{\mathrm{MMSE}} - \mathbf{W}_{\mathrm{RF}}^{(\mathrm{k})}\mathbf{W}_{\mathrm{BB}}^{(\mathrm{k})}\right\|_{\mathrm{F}}}$$

end
$\mathbf{W}_{\mathrm{BB}} = \mathbf{W}_{\mathrm{BB}}^{*}, \mathbf{W}_{\mathrm{RF}} = \mathbf{W}_{\mathrm{RF}}^{*}$

5. Results and Discussions

This section presents the simulation results of the proposed scheme under an Nr × Nt = 16 × 64 mmWave MIMO system. The two types of antenna orientation are considered, namely, uniform planar array (UPA, 8×8 at transmitter and 4×4 at the receiver) and uniform linear array (ULA) with antenna spacing of half the wavelength. The Transmitter and receiver are assumed to a maximum of 6 RF chains and the simulations have been shown for 4 and 6 RF chains. The results are based on the channel model described in [23], which is assumed 6 scattering clusters that are distributed randomly in a scattering environment. Each cluster consists of 8 scatters that are closely located with 5° of angle spread for all 48 scatters. The path gain for each scatterer is obtained from a complex circular symmetric Gaussian distribution with uniformly distributed mean angles and angular spread of 5°. The popular SOMP algorithm [23] for the hybrid beamforming scheme is compared with the proposed hybrid beamforming (ESOMP method) scheme, and the digital beamforming method is included for ease of comparison. All simulation results are the average of more than 100 independent channel realizations.

Fig. 7 and Fig. 8 represent the antenna geometry of UPA at transmitter and receiver. Spacing between the adjacent antenna elements is $\frac{\lambda}{2}$ uniformly. The 2D antenna array is positioned in X-Y plane and the transmission and reception happens in broadside, i.e., in Z direction. The transmitter radiation response of UPA antenna system is exhibited with

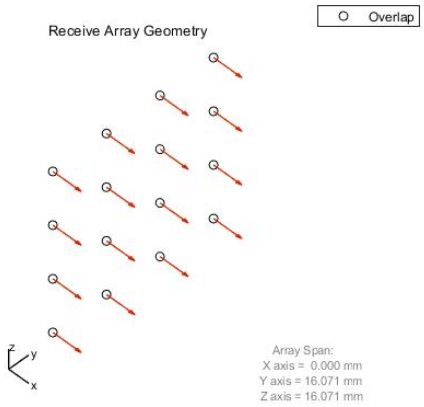

Fig. 8. UPA geometry at MS

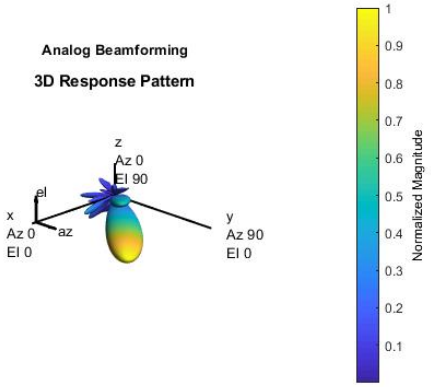

Fig. 9. Radiation response of ABF

respect to analog (Fig. 9) and hybrid beamforming (Fig. 10) techniques.

The analog beamforming produces the radiations in only a single direction which is most dominant. As an ABF can only serve a single user or only a single data stream at a given instant. Hybrid beamforming produces the multiple beams serving multiple users/multiple data streams. fig. 11 and Fig. 12 illustrates the spectral efficiency against the signal-to-noise ratio (SNR) for different algorithms with ULA and UPA antennas respectively.

Fig. 11 captures the spectral efficiency performance for ULA with N_t=64, N_r=16 antenna system, Ns = 4 and Ns =6. The proposed scheme can achieve similar performance with full-digital beamforming. For NS = 6, the proposed method renders the spectral efficiency of 14.2 bits/s/Hz, while the capacity of SOMP is 8.5 bits/s/Hz. Similarly, for Ns=4 and ULA antenna system, the proposed HBF scheme offers a capacity of two times than the SOMP method. Ta-

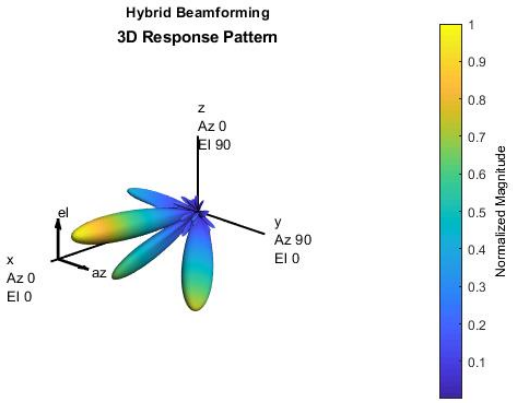

Fig. 10. Radiation response of HBF

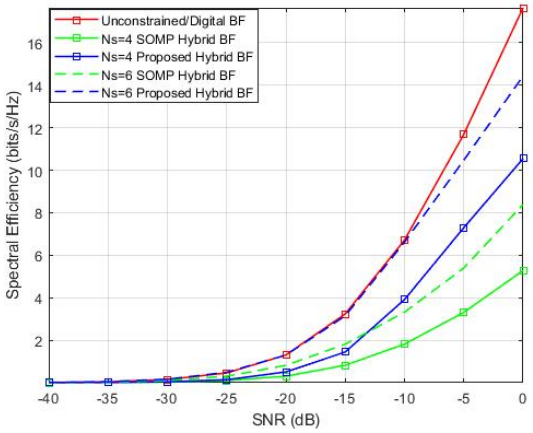

Fig. 11. Spectral efficiency for ULA

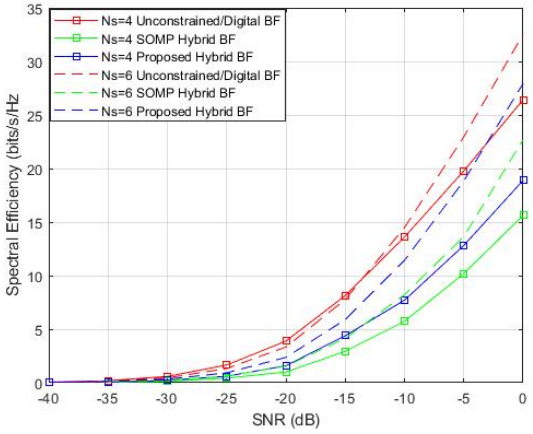

Fig. 12. Spectral efficiency for UPA

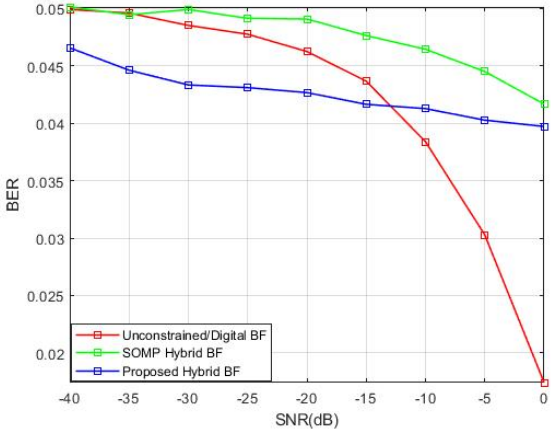

Fig. 13. BER performance for ULA

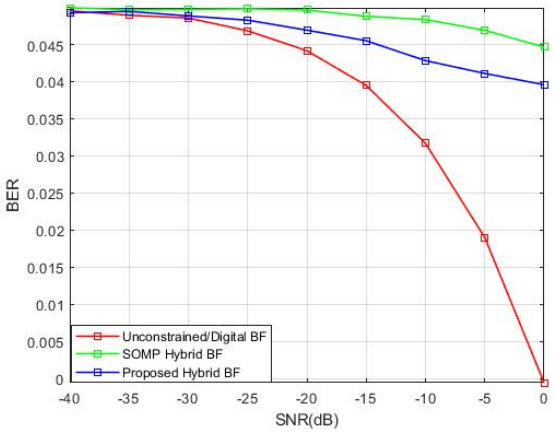

Fig. 14. BER performance for UPA

ble 1 illustrates the comparison of beamforming algorithm in terms of capacity analysis.

Furthermore, Fig. 12 describes the spectral efficiency performance for UPA (16×16 at transmitter and 4×4 at the receiver). The capacity offered by the UPA (16×64 antenna system) antenna system is nearly double that of the ULA (16 antennas). It is evident from Fig. 12 that the proposed method work closer to unconstrained DBF while outperforming the SOMP scheme.

Fig. 13 depicts the BER measurement of a uniform linear array for different beamforming schemes considering a fully connected beamforming structure. As it represents, the proposed HBF scheme produces a better performance than other competing methods such as conventional DBF which does not have constraints like constant modulus that exists in Hybrid beamforming systems. Fig. 14 shows the BER performance comparison for the uniform planar array. Yet it is proved that the proposed scheme is superior to the

Table 1. Performance comparison in terms of system capacity

System Capacity in bits/Sec/Hz				
Data Streams, RF Chains	Antenna Type	Beamforming Techniques		
		DBF	SOMP HBF	Proposed ESOMP HBF
Ns=4, N_t^{RF}=4	ULA (N_t=64, N_r=16)	18	5.2	10.4
	UPA (Tx = 8×8 , Rx = 4×4)	27	16	19
Ns=6, N_t^{RF}=6	ULA (N_t=64, N_r=16)	18	8.5	14.2
	UPA (Tx = 8×8 , Rx = 4×4)	32	23	28

other methods. The BER of the proposed scheme ensures that the ESOMP algorithm is more robust as compared to the existing SOMP method.

6. Conclusions

This paper presents a hybrid beamforming algorithm that produces the optimum precoding and combining weights for mmWave MIMO communications for the downlink scenario. While reducing the hardware complexity, cost, and power consumption, the proposed scheme achieves the improved spectral efficiency and bit error rate performance compared to the SOMP algorithm. Therefore, the scheme proposed in this paper is beneficial and can be employed in the implementation of the multi-user mmWave communication system. This work can be extended further by using non-orthogonal multiple access in combination with mmWave MIMO. The mmWave massive MIMO hybrid beamforming systems improve the performance at a reduced cost. However, the proposed scheme does not address serving multiple users in each beam. Thus, leads to an inadequate number users being served, as the number of users cannot be more than the number of RF chains at a given instant. To further increase the spectrum efficiency, further study reveals the need of combining NOMA with mmWave massive MIMO systems. Therefore, the so-called mmWave massive MIMO-NOMA systems promise to serve multiple users per beam at the same time and frequency by applying superposition coding within the same beam at the transmitter and successive interference cancellation (SIC) at the receivers.

References

[1] S. K. Rao and R. Prasad, (2018) *"Impact of 5G technologies on industry 4.0"* **Wireless personal communications *100***(1): 145–159.

[2] M. L. Attiah, A. A. M. Isa, Z. Zakaria, M. Abdulhameed, M. K. Mohsen, and I. Ali, (2020) *"A survey of mmWave user association mechanisms and spectrum sharing approaches: an overview, open issues and challenges, future research trends"* **Wireless Networks *26***(4): 2487–2514.

[3] X. Wang, L. Kong, F. Kong, F. Qiu, M. Xia, S. Arnon, and G. Chen, (2018) *"Millimeter wave communication: A comprehensive survey"* **IEEE Communications Surveys & Tutorials *20***(3): 1616–1653.

[4] S. A. Busari, K. M. S. Huq, S. Mumtaz, L. Dai, and J. Rodriguez, (2017) *"Millimeter-wave massive MIMO communication for future wireless systems: A survey"* **IEEE Communications Surveys & Tutorials *20***(2): 836–869.

[5] Y. Huo, X. Dong, W. Xu, and M. Yuen, (2019) *"Enabling multi-functional 5G and beyond user equipment: A survey and tutorial"* **IEEE Access *7***: 116975–117008.

[6] R. Méndez-Rial, C. Rusu, N. González-Prelcic, A. Alkhateeb, and R. W. Heath, (2016) *"Hybrid MIMO architectures for millimeter wave communications: Phase shifters or switches?"* **Ieee Access *4***: 247–267.

[7] F. Sohrabi and W. Yu, (2017) *"Hybrid analog and digital beamforming for mmWave OFDM large-scale antenna arrays"* **IEEE Journal on Selected Areas in Communications *35***(7): 1432–1443.

[8] S. Payami, M. Ghoraishi, and M. Dianati, (2016) *"Hybrid beamforming for large antenna arrays with phase shifter selection"* **IEEE Transactions on Wireless Communications *15***(11): 7258–7271.

[9] Y.-Y. Lee, C.-H. Wang, and Y.-H. Huang, (2014) *"A hybrid RF/baseband precoding processor based on parallel-index-selection matrix-inversion-bypass simultaneous orthogonal matching pursuit for millimeter wave MIMO systems"* **IEEE Transactions on Signal Processing *63***(2): 305–317.

[10] X. Yu, J.-C. Shen, J. Zhang, and K. B. Letaief, (2016) *"Alternating minimization algorithms for hybrid precoding in millimeter wave MIMO systems"* **IEEE Journal of Selected Topics in Signal Processing *10***(3): 485–500.

[11] C.-H. Chen, C.-R. Tsai, Y.-H. Liu, W.-L. Hung, and A.-Y. Wu, (2016) *"Compressive sensing (CS) assisted low-complexity beamspace hybrid precoding for millimeter-wave MIMO systems"* **IEEE Transactions on Signal Processing *65***(6): 1412–1424.

[12] C.-C. Yeh, K.-N. Hsu, J.-C. Chi, and Y.-H. Huang. "Adaptive simultaneous orthogonal matching pursuit for mmWave hybrid beam tracking". In: *2018 IEEE 23rd International Conference on Digital Signal Processing (DSP)*. IEEE. 2018, 1–5.

[13] T. Lin, J. Cong, Y. Zhu, J. Zhang, and K. B. Letaief, (2019) *"Hybrid beamforming for millimeter wave systems using the MMSE criterion"* **IEEE Transactions on Communications *67***(5): 3693–3708.

[14] M. Li, Z. Wang, H. Li, Q. Liu, and L. Zhou, (2019) *"A hardware-efficient hybrid beamforming solution for mmWave MIMO systems"* **IEEE Wireless Communications *26***(1): 137–143.

[15] W. U. Bajwa, J. Haupt, A. M. Sayeed, and R. Nowak, (2010) *"Compressed channel sensing: A new approach to estimating sparse multipath channels"* **Proceedings of the IEEE *98***(6): 1058–1076.

[16] G. Lee, J. Park, Y. Sung, and J. Seo. "A new approach to beamformer design for massive MIMO systems based on k-regularity". In: *2012 IEEE Globecom Workshops*. IEEE. 2012, 686–690.

[17] S. Sun, T. S. Rappaport, M. Shafi, P. Tang, J. Zhang, and P. J. Smith, (2018) *"Propagation models and performance evaluation for 5G millimeter-wave bands"* **IEEE Transactions on Vehicular Technology *67***(9): 8422–8439.

[18] T. E. Bogale, L. B. Le, A. Haghighat, and L. Vandendorpe, (2016) *"On the number of RF chains and phase shifters, and scheduling design with hybrid analog–digital beamforming"* **IEEE Transactions on Wireless Communications *15***(5): 3311–3326.

[19] A. F. Molisch, V. V. Ratnam, S. Han, Z. Li, S. L. H. Nguyen, L. Li, and K. Haneda, (2017) *"Hybrid beamforming for massive MIMO: A survey"* **IEEE Communications magazine *55***(9): 134–141.

[20] A. N. Uwaechia and N. M. Mahyuddin, (2020) *"A comprehensive survey on millimeter wave communications for fifth-generation wireless networks: Feasibility and challenges"* **IEEE Access *8***: 62367–62414.

[21] C. Yu, J. Jing, H. Shao, Z. H. Jiang, P. Yan, X.-W. Zhu, W. Hong, and A. Zhu, (2019) *"Full-angle digital predistortion of 5G millimeter-wave massive MIMO transmitters"* **IEEE Transactions on Microwave Theory and Techniques *67***(7): 2847–2860.

[22] O. El Ayach, S. Rajagopal, S. Abu-Surra, Z. Pi, and R. W. Heath, (2014) *"Spatially sparse precoding in millimeter wave MIMO systems"* **IEEE transactions on wireless communications *13***(3): 1499–1513.

[23] S. Haghighatshoar and G. Caire. "Enhancing the estimation of mm-Wave large array channels by exploiting spatio-temporal correlation and sparse scattering". In: *WSA 2016; 20th International ITG Workshop on Smart Antennas*. VDE. 2016, 1–7.